Acta Crystallographica Section B
Structural Science
ISSN 0108-7681

Structures of potassium, sodium and lithium bis(oxalato)borate salts from powder diffraction data

Peter Y. Zavalij,* Shoufeng Yang and M. Stanley Whittingham

Chemistry Department and Institute for Materials Research, State University of New York at Binghamton, Binghamton, NY 13902-6000, USA

Correspondence e-mail: zavalij@binghamton.edu

Received 20 June 2003
Accepted 9 October 2003

The crystal structures of the alkali-metal bis(oxalato)borate salts $A[B(C_2O_4)_2]$ (A = K, Na, Li) have been determined *ab initio* using powder diffraction data obtained from a laboratory diffractometer. The K compound crystallizes in the orthorhombic space group *Cmcm* and its structure has been solved by direct methods applied to the integrated intensities from full pattern decomposition. The Na compound is isostructural with the K salt, while the crystal structure of the highly hydroscopic Li compound differs from the other two. It has an orthorhombic lattice, space group *Pnma*, and its structure was solved by the global optimization method using a parallel tempering approach. In the K and Na structures the metal ions and complex borate ions form chains with *m*2*m* symmetry. Metal–oxygen bonding between the chains links them into a layer and then a framework with square tunnels. The coordination number of both K and Na is eight. The Li compound also contains chains that have *.m.* symmetry and are bound together into a three-dimensional framework. The coordination polyhedron of the Li atom is a square pyramid with Li lying in its base. This square pyramidal coordination leads to its high reactivity with moisture to give $Li[B(C_2O_4)_2]H_2O$ with lithium in six coordination.

1. Introduction

Over the last decade research aimed at improving existing materials used in lithium rechargeable batteries and the search for new materials has been constantly growing. This is because of the increasing everyday use of these batteries and the need to improve such properties as lifetime (cyclability) and weight (capacity), as well as to lower their cost and increase their safety. It is known that the performance of the battery does not depend solely on the properties of the electrode materials, but also on other components such as, for example, the electrolyte that consists of organic solvent and a lithium salt. Among the latter, commonly used lithium salts are perchlorate $LiClO_4$, hexafluoroarsenate $LiAsF_6$ and hexafluorophosphate $LiPF_6$, as well as tetrafluoroborate $LiBF_4$. The first salt can cause explosions in a mixture with organic substances; the second is poisonous; others are also not desirable owing to the presence of fluorine. Therefore, a better lithium salt is always under consideration. Recently, the novel lithium bis(oxalato)borate (LiBOB), $LiB(C_2O_4)_2$, was described (Xu & Angell, 2001) and patented as a conducting salt for lithium-ion batteries (Wietelmann *et al.*, 1999, 2003). However, its crystal structure was not reported, nor were other BOB compounds described.

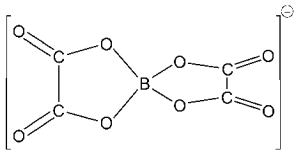

In this work, the crystal structures of LiBOB along with the two other alkali metal salts NaBOB and KBOB have been determined from powder data.

2. Experimental

2.1. Synthesis

$H_2C_2O_4{\cdot}2H_2O$, H_3BO_3 and $LiOH{\cdot}H_2O$ were separately dissolved in water and then mixed in a molar ratio of 2:1:1. The LiOH solution was added slowly to the acidic mixture with vigorous stirring. The turbid solution was heated in an oil bath at 393 K until dry. The crude product was heated in a vacuum oven at 453 K for 2 h. After cooling to room temperature, the sample was dissolved in hot acetonitrile and any impurities were filtered out. The white product obtained was recrystallized and the powder was dried in a vacuum oven at 373 K for 24 h (Xu & Angell, 2001). The LiBOB thus obtained, in the form of a fine powder, is highly hygroscopic and on exposure to air reversibly transforms into the monohydrate $LiB(C_2O_4)_2{\cdot}H_2O$. This was confirmed by thermogravimetric analysis.

The Na and K compounds were synthesized in a similar way. These two salts are not soluble in acetonitrile nor in many other solvents. To purify the products, they were dispersed in hot acetonitrile solution. The undissolved white powder was collected on a filter paper and dried at 363 K in a vacuum oven for 12 h. The white polycrystalline products NaBOB and KBOB are stable in air and do not react with moisture.

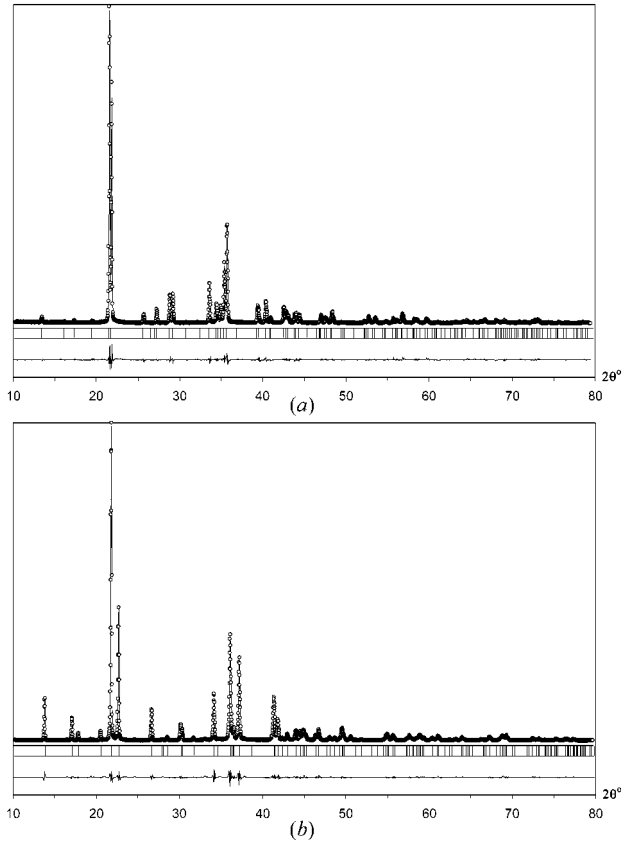

Figure 1
Observed (small circles), calculated (solid line) and difference (bottom) plots from Rietveld refinement of (*a*) $KB(C_2O_4)_2$ and (*b*) $NaB(C_2O_4)_2$. Vertical lines indicate the positions of the reflections.

2.2. Crystal structure determination

The relatively low crystallinity of LiBOB (peak width ranges from 0.15 to 0.30° in 2θ) and the pseudo-hexagonal relationship of its cell dimensions, as will be discussed further, reduce the chances of *ab initio* structure determination from the powder data. Therefore, many attempts to grow single crystals of LiBOB were made. The highly soluble LiBOB was recrystallized from a variety of solvents that yielded large crystals that included solvent or a fine powder of the unsolvated material. Thus, single-crystal experiments were performed on a wide range of solvates with water, acetonitrile, acetone, dimethoxyethane, 1,3-dioxolane and ethylene carbonate. These results are reported elsewhere (Yang *et al.*, 2003).

2.2.1. Data collection and indexing. The powder diffraction data were collected at room temperature using Cu $K\alpha$ radiation on a laboratory Scintag XDS2000 powder diffractometer equipped with a Ge(Li) solid-state detector: step scan method, step size 0.02° 2θ, counting time 8–12 s per step for KBOB and NaBOB (Fig. 1) and 2 s per step for LiBOB (Fig. 2*a*). In order to determine the interaction of LiBOB with water in air, to confirm its purity and test its thermal stability, a powder pattern was recorded at 423 K (Fig. 2*b*) on a Philips PW3040 powder diffractometer equipped with curved graphite monochromator, proportional detector and high-temperature stage.

The powder patterns were indexed by the *ITO* (Visser, 1969) and *TREOR* (Werner *et al.*, 1985) programs using peak positions obtained from the profile fitting. The K and Na compounds yield similar unit-cell dimensions and a C-centered orthorhombic lattice. Unambiguous reflection conditions indicated the space group *Cmcm* or one of its non-centrosymmetric subgroups $Cmc2_1$ or $C2cm$ ($Ama2$).

Indexing of the LiBOB pattern was much more challenging. Initially, a room-temperature pattern was indexed in the hexagonal lattice with no special reflection conditions and cell dimensions a = 15.194 (4) and c = 6.362 (2) Å. This solution had a high indexing figure of merit F_{20} = 58 with 26 possible reflections for 23 observed peaks. However, multiple attempts to solve the structure using global optimization and direct methods failed even when using space groups with the lowest hexagonal and trigonal symmetry. It was noticed that all models of the crystal structure yielded a high intensity for the (100) reflection, whose diffraction peak was not observed

along with a few more peaks in the low-angle region. Thus, it was assumed that the lattice symmetry might be lower than hexagonal and another indexing solution was tested. The second option on the *TREOR* indexing list was an orthorhombic cell with a slightly lower figure of merit $F_{20} = 54$ with 37 possible reflections for the 23 observed peaks. The primitive orthorhombic cell obtained is related to the hexagonal one as

$$a_{\rm ort} = c_{\rm hex},\ b_{\rm ort} = a_{\rm hex}/2,\ \text{and}\ c_{\rm ort} = 3^{1/2} \cdot a_{\rm hex}/2.$$

This is not simply a representation of the hexagonal cell in a base-centered orthorhombic cell with twice the volume, but a primitive orthorhombic cell with a volume which is half that of the hexagonal cell. The greater number of possible reflections in the orthorhombic cell is because of the special relationship between the cell dimensions. It is obvious from Fig. 2(*b*) that the ratio of the number of observed peaks to the number of possible reflections (not counting overlapped) is much better for the orthorhombic than for the hexagonal indexing. The final cell parameters refined by full profile fitting are a = 6.3635 (4), b = 7.5998 (3), c = 13.1715 (9) Å, V = 636.99 (6) Å^3 for the data recorded at room temperature and a = 6.3425 (2), b = 7.6359 (2), c = 13.1667 (4) Å, V = 637.67 (3) Å^3 at 423 K.

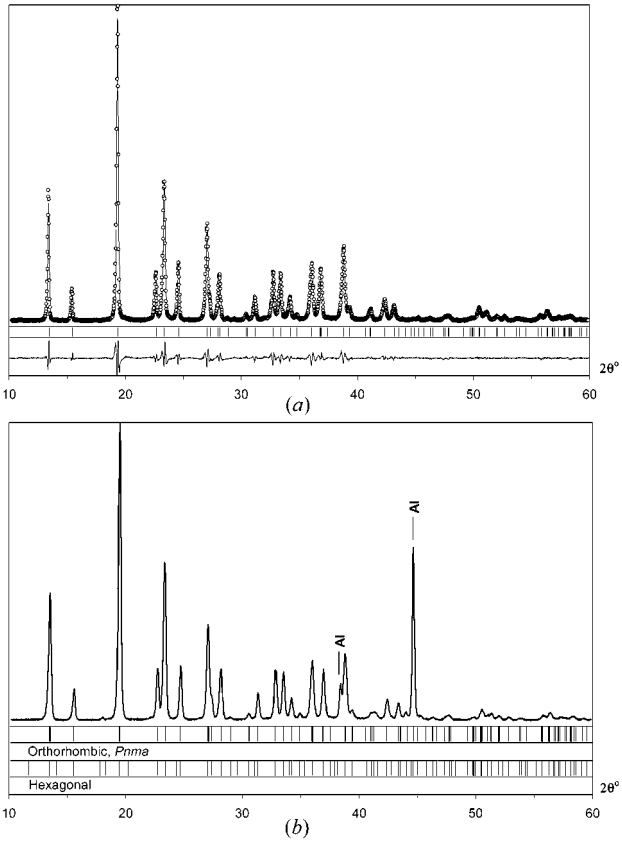

Figure 2
(*a*) Observed, calculated and difference plots from Rietveld refinement for $LiB(C_2O_4)_2$ at room temperature; (*b*) experimental powder pattern of $LiB(C_2O_4)_2$ measured at 423 K with calculated positions of the reflections for the correct orthorhombic cell (upper) and the incorrect hexagonal cell (lower).

The space-group determination for LiBOB was also not unambiguous because of peak overlap caused by the pseudo-hexagonal relationship between the cell parameters. Three possible centrosymmetric space groups were deduced based on the reflection conditions: $k + l = 2n$ for $0kl$ reflections and no conditions for $h0l$ reflections. Conditions for $hk0$ reflections could not be determined unambiguously owing to the peak overlap. These are *Pnmm*, *Pnmn* and *Pnma*. Rather than testing all of them separately, their common non-centrosymmetric subgroup $Pnm2_1$ was used in the structure solution, as will be discussed further.

2.2.2. Structure determination and refinement. The crystal structure of KBOB was solved by direct methods using *WinCSD* (Akselrud *et al.*, 1993) software from the integrated intensities of 161 peaks obtained by Pawley full pattern decomposition (Pawley, 1981) using the Materials Studio (2001). The E-map from the best solution revealed the positions of the K ion and most of the light atoms of the BOB ion. Missing atoms were located from difference-Fourier maps.

Taking into account the same symmetry, similar cell dimensions and similar powder patterns (Fig. 1), the structure of NaBOB was assumed to be isostructural to KBOB and that was confirmed by Rietveld refinement (Rietveld, 1969).

The structure determination of the LiBOB using a reciprocal space approach such as Patterson or direct methods was not even attempted. The relatively broad peaks along with the highly overlapped reflections, because of the accidental pseudo-hexagonal relationship of the cell dimensions (see §2.2.1), would make success very difficult if not impossible. Therefore, the direct space approach realised in *FOX* software (Favre-Nicolin & Cerny, 2002) was used, which employs global optimization of the crystal structure. Multiple structure models were generated by Monte-Carlo methods in simulated annealing or parallel tempering approaches. The latter two imply that the new model is not completely random, but is somehow related to the best structure known at the moment. In other words, the new structure should be within some specified range (distance in multi-dimensional space of varying parameters) from the best-known structure. The cost function in the case of powder diffraction data is the difference between the observed and calculated profile expressed as an integrated weighted R factor.

The structure solution of LiBOB was performed in the space group $Pnm2_1$ using the unit cell and profile parameters from the Pawley full profile fitting. Building blocks were defined as BOB ions with fixed geometry, but variable position and orientation, and independent Li atoms, which resulted in nine optimized parameters. The optimization converged with integrated $R_{\rm wp}$ = 0.18, yielding a geometrically reasonable model with BOB residing in the mirror plane. The coordination polyhedron of Li was also acceptable. Nevertheless, the Li position was additionally confirmed from the difference-Fourier map and was unambiguously predicted geometrically assuming the location of the BOB ions was known. Analysis of the crystal structure in the non-centrosymmetric space group

Table 1
Experimental details.

	KBOB	NaBOB	LiBOB
Crystal data			
Chemical formula	C_4BKO_8	C_4BNaO_8	C_4BLiO_8
M_r	225.96	209.85	193.79
Cell setting, space group	Orthorhombic, *Cmcm*	Orthorhombic, *Cmcm*	Orthorhombic, *Pnma*
a, b, c (Å)	8.26990 (11), 11.0102 (3), 8.16917 (11)	8.12756 (8), 10.3399 (2), 7.82108 (10)	6.3635 (4), 7.5998 (3), 13.1715 (9)
V (Å^3)	743.83 (2)	657.27 (2)	636.99 (6)
Z	4	4	4
D_x (Mg m^{-3})	2.018	2.121	2.021
Radiation type	Cu $K\alpha_1$, Cu $K\alpha_2$	Cu $K\alpha_1$, Cu $K\alpha_2$	Cu $K\alpha_1$, Cu $K\alpha_2$
Temperature (K)	295	295	295
Specimen form, colour	Cylinder (particle morphology: plate-like), white	Cylinder (particle morphology: plate-like), white	Flat sheet (particle morphology: plate-like), white
Specimen size (mm)	25 × 25 × 1	25 × 25 × 1	25 × 25 × 1
Specimen preparation pressure (kPa)	Ambient	Ambient	Ambient
Specimen preparation temperature (K)	295	295	295
Data collection			
Diffractometer	Scintag XDS2000 powder diffractometer	Scintag XDS2000 powder diffractometer	Scintag XDS2000 powder diffractometer
Data collection method	Specimen mounting: packed powder pellet; mode: reflection; scan method: step	Specimen mounting: packed powder pellet; mode: reflection; scan method: step	Specimen mounting: packed powder pellet; mode: reflection; scan method: step
2θ (°)	$2\theta_{min}$ = 10.02, $2\theta_{max}$ = 79.48, increment = 0.02	$2\theta_{min}$ = 10.02, $2\theta_{max}$ = 80.98, increment = 0.02	$2\theta_{min}$ = 10.0, $2\theta_{max}$ = 59.98, increment = 0.02
Refinement			
Refinement on	Y_{obs}	Y_{obs}	Y_{obs}
R factors and goodness of fit	R_p = 0.072, R_{wp} = 0.097, R_{exp} = 0.040, S = 2.45	R_p = 0.069, R_{wp} = 0.100, R_{exp} = 0.031, S = 3.26	R_p = 0.094, R_{wp} = 0.118, R_{exp} = 0.051, S = 2.35
Profile function	CW Profile function number 3 with 19 terms; pseudovoigt profile coefficients as parameterized in Thompson *et al.* (1987); asymmetry correction of Finger *et al.* (1994); peak tails are ignored where the intensity is below 0.0010 times the peak	CW Profile function number 3 with 19 terms; pseudovoigt profile coefficients as parameterized in Thompson *et al.* (1987); asymmetry correction of Finger *et al.* (1994); peak tails are ignored where the intensity is below 0.0020 times the peak	CW Profile function number 3 with 19 terms; pseudovoigt profile coefficients as parameterized in Thompson *et al.* (1987); asymmetry correction of Finger *et al.* (1994); peak tails are ignored where the intensity is below 0.0050 times the peak
No. of parameters	59	48	47
Weighting scheme	$w = 1/Y_{obs}(i)$	$w = 1/Y_{obs}(i)$	$w = 1/Y_{obs}(i)$
$(\Delta/\sigma)_{max}$	0.03	0.06	0.04
Preferred orientation correction	Spherical harmonic ODF − spherical harmonic order = 4; preferred orientation correction range: min = 0.793, max = 1.461	Spherical harmonic ODF − spherical harmonic order = 4; preferred orientation correction range: min = 0.728, max = 1.279	Spherical harmonic ODF − spherical harmonic order = 4; preferred orientation correction range: min = 0.897, max = 1.067

Computer programs used: *DMSNT* (Scintag Inc., 1999), *WinCSD* (Akselrud *et al.*, 1993), *SHELXS* (Sheldrick, 1990), *FOX* (Favre-Nicolin & Cerny, 2002), *GSAS* (Larson & Von Dreele, 2000), *ATOMS* (Dowty, 1999); *EXPGUI* (Toby, 2001).

clearly points to the centrosymmetric *Pnma* group, which was confirmed by *PLATON* software (Spek, 2003) and further structure refinement.

The Rietveld refinement of all compounds was conducted using *GSAS* (Larson & Von Dreele, 2000) and *EXPGUI* (Toby, 2001) software, as summarized in Table 1.[1] Absorption and porosity effects were corrected using the Suortti (1972) approximation. The anisotropy and complexity of the particle's shape yielded the strong preferred orientation, which was refined using the spherical harmonics approach (Von Dreele, 1997). This effect is usually observed when particles have quite different dimensions in all three directions, *e.g.* a ribbon-like shape, and requires defining at least two preferred orientation axes or using a more complex approach (Pecharsky & Zavalij, 2003). Both KBOB and NaBOB samples exhibit strong preferred orientation effects, but it was especially severe for the K compound. Therefore, extra care was taken in sample preparation in order to experimentally minimize the preferred orientation effects on intensity, which included thorough grinding, side filling and spinning of the sample. In both cases the preferred orientation was refined up to fourth order for the spherical harmonics, yielding a maximum correction around 1.8. This is several times less than the correction needed for improperly prepared samples. The preferred

[1] Supplementary data for this paper are available from the IUCr electronic archives (Reference: TA5002). Services for accessing these data are described at the back of the journal.

Table 2
Statistics of distances (Å) and angles (°) for the BOB ion from powder and single-crystal data.

Average powder data: distances were constrained during the refinement from powder data.

	Powder data		Single-crystal data (Yang *et al.* (2003)	
Distance/angle	Average	Min–max	Average	Min–max
B—O	1.474	1.460–1.495	1.471	1.446–1.502
C—C	1.538	1.512–1.544	1.530	1.508–1.557
C═O	1.198	1.187–1.206	1.203	1.191–1.229
C—O	1.326	1.319–1.341	1.324	1.298–1.345
O—B—O	109.5	102.6–111.8	109.5	104.8–113.1
O═C—O	127.4	125.4–130.2	126.6	123.9–128.4
O═C—C	124.5	122.0–126.7	125.5	122.6–128.0
O—C—C	108.0	106.4–110.7	107.8	106.3–110.5

orientation for the LiBOB sample was treated the same way, yet it was noticeably lower (Table 1).

The structure refinement yielded a noticeable deviation in the geometry of the BOB ions compared with the single-crystal data (Yang *et al.*, 2003) owing to the still significant preferred orientation in KBOB and NaBOB, and the high degree of overlapping in LiBOB. Nonetheless, an initially unconstrained refinement was performed to confirm all the atoms and only then were soft constraints on the B—O, C—C, C—O and C═O bond lengths applied. Angles were not constrained and were used as a reliability criteria. The constraints resulted in a stable refinement and quite good agreement in C—C—O, C—C═O, O═C—O and O—B—O angles, as illustrated in Table 2, where the dimensions from this work are compared between themselves and with single-crystal data. Individual atomic displacement parameters (U_{iso}) for the KBOB and NaBOB structures refined independently fall in the range 0.02–0.035 Å^2. This confirms the correctness of the model and constraints used. In the case of LiBOB the isotropic parameters were kept common for all atoms.

A Rietveld refinement of the LiBOB from experimental data measured at 423 K was also undertaken and resulted in essentially the same structure as that at room temperature. Nonetheless, it yielded no improvement in the refinement because of an increase in the peak-width from 0.15–0.30° 2θ at room temperature to 0.25–0.35° 2θ at 423 K.

2.3. Results and discussion

This is the first structural characterization of the bis(oxalato)borate ion. The Na and K compounds appear to be isostructural. The only noticeable difference between them is a deformation of the Na and K coordination polyhedra owing to the different atomic radii. The Li structure differs substantially from the other two.

Both the Na and K ions have 6 + 2 coordination. This includes four O atoms from two opposite chelating BOB ions that are mutually perpendicular to each other. Each BOB ion coordinates two metals with its opposite oxalate groups, forming an infinite chain along *b* as shown in Fig. 3. The other two ligands are terminal O1 atoms from neighboring chains binding them into a layer as shown in Fig. 3(*a*). These six oxygen ions are at about the same distance to the metal ion which is ∼2.77 Å for K and ∼2.50 Å for Na. However, there are two more bonds formed by O3 atoms that bind the layers into a framework, as shown in Fig. 3(*b*). The lengths of these bonds exceed 3 Å, which makes them much weaker compared with the main *M*—O bonds (Table 3). The BOB ion is linked to six metal atoms: chelating two metal ions along the chain and forming two strong and two weak bonds with atoms from other chains. The local symmetry of the BOB ion is $\bar{4}m2$, but only *m*2*m* is realised in the K and Na structures. The metal ions also lie on the intersection of two mirror planes that coincides with the symmetry of the BOB ions and results in

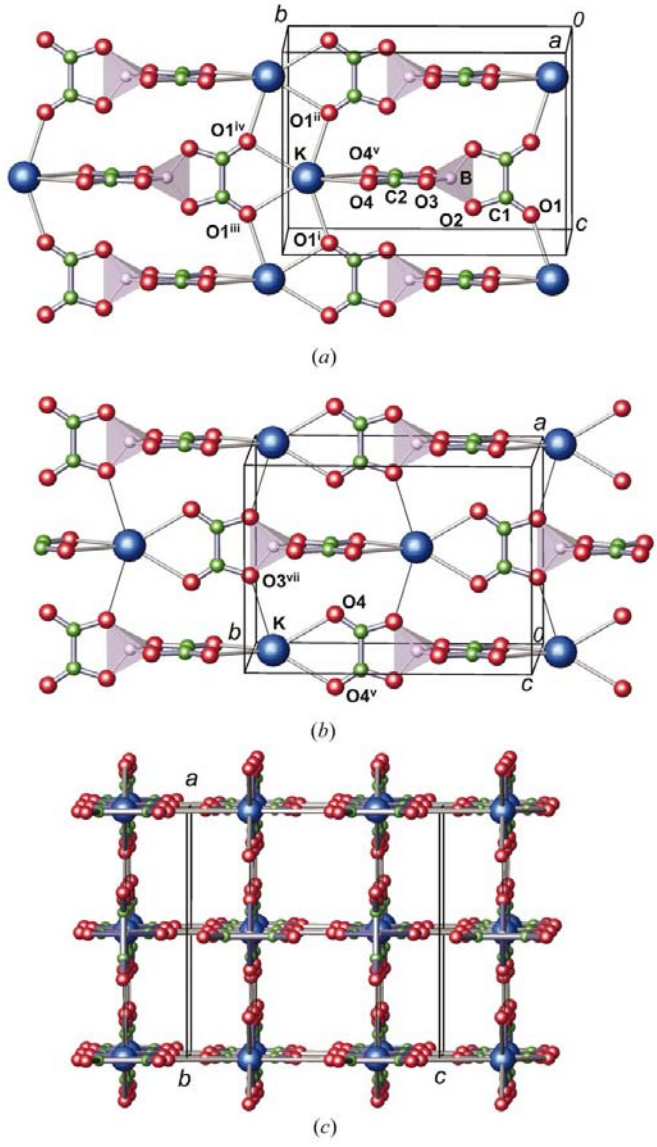

Figure 3
Crystal structure of $KB(C_2O_4)_2$: (*a*) (100) layer of strongly bonded chains; (*b*) (001) layer of weakly bonded chains; (*c*) framework shown along the *b* axis. K is shown as large blue spheres, B as small spheres inside semi-transparent tetrahedra, O and C as red and green spheres. The thin lines in (*b*) indciate weak K—O interactions. The symmetry codes are as given in Table 3.

Table 3
Selected distances (Å) and angles (°) in K, Na and Li coordination polyhedra.

KBOB		NaBOB		LiBOB	
K—O1^{i}	2.745 (4)	Na—O1^{i}	2.532 (3)	Li—O6^{ii}	1.94 (3)
K—O1^{iii}	2.745 (4)	Na—O1^{iii}	2.532 (3)	Li—O4^{iv}	2.02 (3)
K—O1^{v}	2.774 (5)	Na—O1^{v}	2.486 (3)	Li—O4^{ii}	2.11 (3)
K—O1^{vi}	2.774 (5)	Na—O1^{vi}	2.486 (3)	Li—O2^{vii}	2.315 (6)
K—O4	2.777 (5)	Na—O4	2.490 (3)	Li—O2^{viii}	2.315 (6)
K—O4^{ix}	2.777 (5)	Na—O4^{ix}	2.490 (3)	Li···O3	3.01 (4)
K—O3^{x}	3.106 (4)	Na—O3^{x}	3.025 (2)		
K—O3^{xi}	3.106 (4)	Na—O3^{xi}	3.025 (2)		
O1^{v}—K—O1^{vi}	63.8 (2)	O1^{v}—Na—O1^{vi}	71.52 (14)	O2^{vii}—Li—O2^{viii}	170.5 (16)
O4—K—O4^{ix}	62.5 (2)	O4—Na—O4^{ix}	69.94 (13)	O4^{iv}—Li—O6^{ii}	155.2 (18)
				O4^{ii}—Li—O6^{ii}	89.5 (12)
K—K^{xii}	4.361 (2)	Na—Na^{xii}	4.157 (2)	Li—Li^{iv}	3.74 (4)
K—K^{xiii}	4.361 (2)	Na—Na^{xiii}	4.157 (2)	Li—Li^{xiv}	3.74 (4)

Symmetry codes: (i) $x, 1-y, \frac{1}{2}+z$; (ii) $1+x, y, z$; (iii) $x, 1-y, 1-z$; (iv) $\frac{1}{2}+x, \frac{1}{2}-y, \frac{1}{2}-z$; (v) $-x, 1+y, \frac{3}{2}-z$; (vi) $x, 1+y, z$; (vii) $1-x, -y, 1-z$; (viii) $1-x, \frac{1}{2}+y, 1-z$; (ix) $-x, y, z$; (x) $-\frac{1}{2}+x, \frac{1}{2}+y, z$; (xi) $\frac{1}{2}-x, \frac{1}{2}+y, z$; (xii) $x, 2-y, \frac{1}{2}+z$; (xiii) $x, 2-y, -\frac{1}{2}+z$; (xiv) $-\frac{1}{2}+x, \frac{1}{2}-y, \frac{1}{2}-z$.

the arrangement of an interesting framework with square tunnels along the *b* axis, as shown in Fig. 3(*c*).

The lithium bis(oxalato)borate structure consists of one-dimensional chains lying in the mirror plane (Fig. 4*a*).

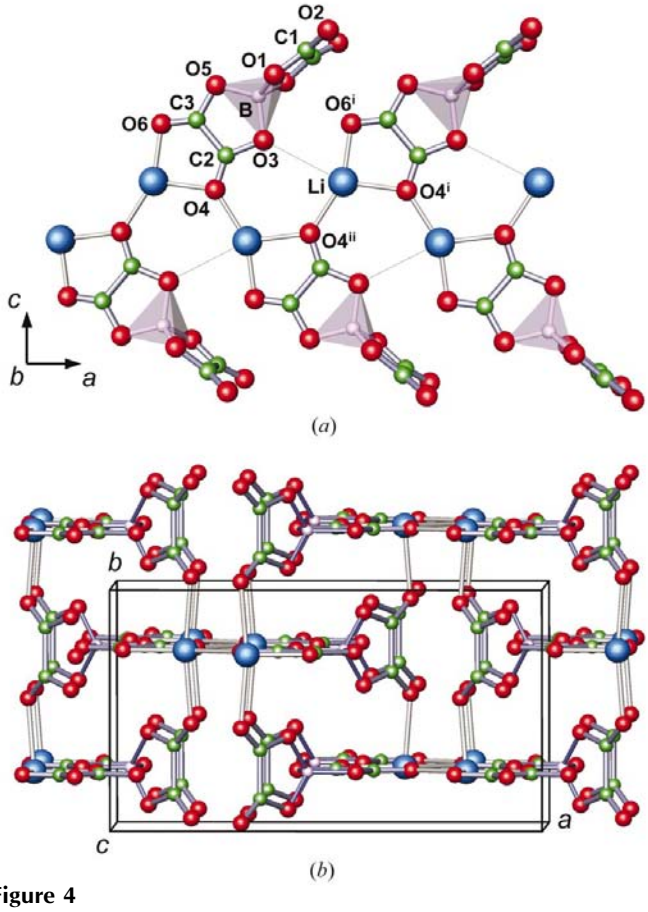

Figure 4
(*a*) $Li(C_2O_4)_2$ chain with additional Li···O contacts shown as thin lines; (*b*) framework shown as the stacking of the chains linked with vertical Li—O bonds. Symmetry codes are the same as in Table 3.

However, the smaller size of the Li ion leads to chains and consequently a framework that is quite different from that found in the Na and K structures. The BOB ion also behaves differently. One oxalate group (O4 and O6) chelates lithium in the chain, while another (O2) is bridging the Li atoms from upper and lower chains, as depicted in Fig. 4(*b*). The O4 atom forms an additional bond to form a chain along the *a* axis. The lengths of the Li—O bonds in the chain (Table 3) lie within the range 1.9–2.1 Å, whilst the Li—O2 bonds that link the chains into the framework are noticeably weaker. Thus, five-coordinated Li forms a square pyramid with the O4^{i} atom in its apex and the Li atom only slightly shifted from its base. The position opposite to the apex is occupied by the O3 atom at a distance greater than 3 Å, thus yielding an additional weak interaction along the chain.

Note that the O4^{i}—Li—O6^{i} angle [symmetry code: (i) x, $1-y, +z$], where both O atoms belong to the chelating oxalate group, is near 90° and the corresponding Li—O distances fall in the typical range. This makes the oxalate group an excellent ligand for Li and three such groups could create an octahedral environment for the Li. However, it is not achieved in the title compound probably because of the steric effects of the large and rigid BOB ion. Nevertheless, in most of the LiBOB solvates (Yang *et al.*, 2003) Li has a regular octahedral coordination where one or two corners are occupied by the solvent molecule. The presence of the five-coordinated Li atom in this compound explains the unsuccessful attempts to prepare unsolvated LiBOB by solution chemistry. Tetrahedral coordination of the Li atom with Li—O distances just slightly below 2.0 Å is also sometimes observed, as for example with ethylene carbonate.

Financial support by the National Science Foundation, DMR 0313963, and by the US Department of Energy, Office of Freedom CAR and Vehicle Technologies, through the BATT program at Lawrence Berkeley National Laboratory is greatly appreciated.

References

Akselrud, L. G., Zavalij, P. Y., Grin, Yu. N., Pecharsky, V. K., Baumgartner, B. & Wolfel, E. (1993). *Mater. Sci. Forum*, **133–136**, 335–340.

Dowty, E. (1999). *ATOMS for Windows and Macintosh*, Version 5. Shape Software, 521 Hidden Valley Road, Kingsport, TN 37663, USA.

Favre-Nicolin, V. & Cerny, R. (2002). *J. Appl. Cryst.* **35**, 734–743.

Finger, L. W., Cox, D. E. & Jephcoat, A. P. (1994). *J. Appl. Cryst.* **27**, 892–900.

Larson, A. C. & Von Dreele, R. B. (2000). *General Structure Analysis System* (*GSAS*). Los Alamos National Laboratory Report LAUR 86–748, Los Alamos, New Mexico, USA.
Materials Studio (2001). Accelrys Inc., San Diego, CA.
Pawley, G. S. (1981). *J. Appl. Cryst.* **14**, 357–361.
Pecharsky, V. K. & Zavalij, P. Y. (2003). *Fundamentals of Powder Diffraction and Structural Characterization of Materials.* Dordrecht, The Netherlands: Kluwer Academic Publishers.
Rietveld, H. M. (1969). *J. Appl. Cryst.* **2**, 65–71.
Scintag Inc. (1999). *DMSNT*. Version 1.37. Scintag Inc., Cupertino, CA, USA.
Sheldrick, G. M. (1990). *Acta Cryst.* A**46**, 467–473.
Spek, A. L. (2003). *J. Appl. Cryst.* **36**, 7–13.
Suortti, P. (1972). *J. Appl. Cryst.* **5**, 325–331.
Toby, B. H. (2001). *J. Appl. Cryst.* **34**, 210–213.
Thompson, P., Cox, D. E. & Hastings, J. B. (1987). *J. Appl. Cryst.* **20**, 79–83.
Visser, J. W. (1969). *J. Appl. Cryst.* **2**, 89–95.
Von Dreele, R. B. (1997). *J. Appl. Cryst.* **30**, 517–525.
Werner, P.-E., Eriksson, L. & Westdahl, M. (1985). *J. Appl. Cryst.* **18**, 367–370.
Wietelmann, U., Lischka, U. & Wegner, M. (1999). German Patent DE 19829030 C1.
Wietelmann, U., Lischka, U. & Wegner, M. (2003). United States Patent 6,506,516 .
Xu, W. & Angell, C. A. (2001). *Electrochem. Solid-State Lett.* **4**, E1–E4.
Yang, S., Zavalij, P. Y. & Whittingham, M. S. (2003). In preparation.